Exact solution of the geometrically frustrated spin-$\frac{1}{2}$ Ising-Heisenberg model on the triangulated kagome (triangles-in-triangles) lattice

Jozef Strečka,[*] Lucia Čanová, and Michal Jaščur

Department of Theoretical Physics and Astrophysics, Faculty of Science, P. J. Šafárik University,
Park Angelinum 9, 040 01 Košice, Slovak Republic

Masayuki Hagiwara

KYOKUGEN (Center for Quantum Science and Technology under Extreme Conditions), Osaka University,
1-3 Machikaneyama, Toyonaka, Osaka 560-8531, Japan

The geometric frustration of the spin-1/2 Ising-Heisenberg model on the triangulated kagome (triangles-in-triangles) lattice is investigated within the framework of an exact analytical method based on the generalized star-triangle mapping transformation. Ground-state and finite-temperature phase diagrams are obtained along with other exact results for the partition function, Helmholtz free energy, internal energy, entropy, and specific heat, by establishing a precise mapping relationship to the corresponding spin-1/2 Ising model on the kagome lattice. It is shown that the residual entropy of the disordered spin liquid phase for the quantum Ising-Heisenberg model is significantly lower than for its semiclassical Ising limit ($S_0/N_T k_B = 0.2806$ and 0.4752, respectively), which implies that quantum fluctuations partially lift a macroscopic degeneracy of the ground-state manifold in the frustrated regime. The investigated model system has an obvious relevance to a series of polymeric coordination compounds $Cu_9 X_2(cpa)_6$ (X=F,Cl,Br and cpa=carboxypentonic acid), for which we made a theoretical prediction about the temperature dependence of zero-field specific heat.

I. INTRODUCTION

The antiferromagnetic quantum Heisenberg model (AF-QHM) defined on *geometrically frustrated planar lattices* represents a long-standing theoretical challenge due to a rich variety of unusual ground states it exhibits as a result of the mutual interplay between quantum fluctuations and geometric frustration.[1–4] In particular, the extensive theoretical studies of the spin-1/2 AF-QHM on the triangular,[5] kagome,[6,7] Shastry–Sutherland,[8] star,[9] checkerboard,[10] square kagome,[11] and other lattices[12] have revealed a great diversity in their ground-state and low-temperature behavior. It is now widely accepted that the ground state of the spin-1/2 AF-QHM on some geometrically frustrated planar lattices such as a triangular lattice is the Néel-type ordered state,[5] while there is a still controversial debate on whether[6] or not[7] the disordered spin liquid state is the true ground state of this model on kagome lattice. Anyway, the macroscopic degeneracy of the ground-state manifold turns out to be strongly related to a geometric topology of the underlying lattice, and it is therefore of particular research interest to explore a connection between the zero-point entropy and the lattice geometry.

Another striking feature, which currently attracts a great deal of attention to the spin-1/2 AF-QHM on the geometrically frustrated planar lattices, is the presence of quantized magnetization plateaus in their low-temperature magnetization curves.[2,3] It is worthwhile to remark that this outstanding quantum phenomenon has already been experimentally observed in several prototypical examples of the frustrated quantum spin systems such as the triangular lattice compounds $CsFe(SO_4)_2$,[13] Cs_2CuBr_4,[14] and $RbFe(MoO_4)_2$,[13,15] the kagome lattice compound $[Cu_3(titmb)_2(CH_3COO)_6]\cdot H_2O$,[16] and the Shastry–Sutherland lattice compounds $SrCu_2(BO_3)_2$ (Ref. 17) and RB_4 (R=Er, Tm).[18] It also has been demonstrated that the interplay between the geometric frustration and quantum fluctuations might be a driving force for an enhanced magnetocaloric effect emerging during the adiabatic demagnetization.[19] This makes geometrically frustrated spin systems especially promising refrigerant materials in view of reaching temperatures in the sub-Kelvin range, since they often remain disordered down to the lowest achievable temperatures, unlike paramagnetic salts usually exhibiting a spin-glass transition.

The aforementioned scientific achievements have stimulated an intensive search for inorganic molecular materials, whose paramagnetic metal centers connected in the crystal lattice via superexchange pathways would be strongly frustrated by their geometric arrangement.[20] From this perspective, the series of isostructural polymeric coordination compounds $Cu_9 X_2(cpa)_6 \cdot nH_2O$ (X=F,Cl,Br and cpa=carboxypentonic acid)[21] belongs to the most fascinating geometrically frustrated materials on behalf of a beautiful architecture of their magnetic lattice. The magnetic lattice of this series is built up of divalent copper (Cu^{2+}) ions situated at two crystallographically inequivalent lattice positions (see Fig. 1). Cu^{2+} ions with a square pyramidal coordination (*a* sites) form equilateral triangles (trimers), which are interconnected to one another by Cu^{2+} ions (monomers) with an elongated octahedral coordination (*b* sites). The lattice positions of the *b* sites constitute the regular kagome network, whereas each monomeric *b* site is connected via four bonds to two adjacent trimers of the *a* sites. This magnetic architecture can be accordingly regarded as the triangulated kagome (triangles-in-triangles) lattice, since smaller triangles of the trimeric *a* sites are in fact embedded in larger triangles of the mono-
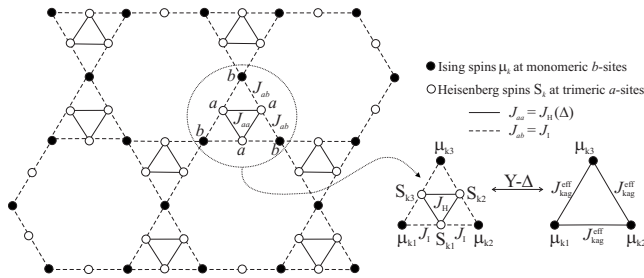
FIG. 1. The cross section of the triangulated kagome (triangles-in-triangles) lattice. The empty and full circles denote lattice positions of the trimeric a sites and monomeric b sites, respectively, which are occupied within the proposed Ising-Heisenberg model by the Heisenberg and Ising spins. The solid and broken lines schematically reproduce the intratrimer Heisenberg interaction $J_{aa} = J_H(\Delta)$ and the monomer-trimer Ising interaction $J_{ab} = J_I$. The ellipse demarcates a six-spin cluster described by Hamiltonian (2), which can be mapped by the use of generalized star-triangle transformation into a simple triangle of the Ising spins mutually interacting via the effective exchange coupling βJ_{kag}^{eff}.

meric b sites forming the basic kagome pattern.

Experimental studies reported on this family of compounds reveal obvious manifestations of the geometric frustration. All three isomorphous compounds do not order down to 1.7 K,[22] the magnetization shows a plateau around one-third of the saturation magnetization, and it does not saturate up to 38 T.[23] Furthermore, the temperature dependence of inverse susceptibility indicates two temperature regimes inherent to two different exchange pathways. The linear dependence of the inverse susceptibility is well fitted by the Curie–Weiss law within the temperature interval between 150 and 250 K with the respective Weiss constants $\Theta_w = -237, -226,$ and -243 K for the fluoro, chloro, and bromo analogs,[22] respectively, while the Weiss constant of the best Curie–Weiss fit generally increases up to roughly $\Theta_w = 6$ K in the temperature range below 50 K.[23] These observations would suggest an extremely high frustration ratio $f = |\Theta_w|/T_c > 130$ (T_c is the ordering temperature)[24] for each member of the $Cu_9X_2(cpa)_6$ family, which makes from this series a prominent class of the highly frustrated materials that possibly display the spin liquid ground state. Based on the considerations of exchange pathways, the strong antiferromagnetic interaction has been assigned to the exchange interaction J_{aa} between the trimeric a sites, while the weaker (possibly ferromagnetic) interaction has been ascribed to the exchange interaction J_{ab} between the trimeric a sites and the monomeric b sites. The overall ratio between both exchange constants might be estimated from the corresponding ratio between the Weiss constants extrapolated from the high- and low-temperature regimes, yielding $|J_{aa}/J_{ab}| \approx 40$.

Motivated by these experiments, Zheng and Sun[25] calculated an exact phase diagram of the spin-1/2 Ising model on the triangulated kagome lattice and the validity of this phase diagram was recently confirmed by an independent exact calculation of Loh *et al.*[26] In addition to the exact ground-state and finite-temperature phase diagrams, the authors of the latter work also presented exact analytical results for several thermodynamic quantities (partition function, Helmholtz free

energy, internal energy, entropy, and specific heat), which were complemented by the Monte Carlo simulations corroborating these exact analytical results and bringing other accurate numerical results for the magnetization and susceptibility in the zero as well as nonzero magnetic field.[26] Among the most interesting findings reported is certainly a theoretical prediction of the spin liquid phase with a large residual entropy per spin $S_0/N_T k_B = \frac{1}{9} \ln 72 = 0.4752$, which appears in the ground state on assumption of a sufficiently strong antiferromagnetic intratrimer interaction $J_{aa}/|J_{ab}| < -1$ (see for details Sec. IVA of Ref. 26).

Unfortunately, the theoretical description based on the Ising model might fail in describing many important vestiges of most of copper-based coordination compounds, since they usually exhibit a rather isotropic magnetic behavior.[27] Besides this, the Ising model description completely disregards the effect of quantum fluctuations, which might play a crucial role in determining the magnetic behavior of coordination compounds incorporating paramagnetic Cu^{2+} ions that have the lowest possible quantum spin number $S = 1/2$. Therefore, the spin-1/2 quantum Heisenberg model is usually thought of as being much more appropriate model for the copper-based coordination compounds.[27] In accordance with this statement, electron-spin-resonance (ESR) measurements performed on the $Cu_9X_2(cpa)_6$ series have shown just a minor anisotropy in the g factor that also serves in evidence of a negligible magnetic anisotropy.[23,28]

Of course, the spin-1/2 quantum Heisenberg model is very difficult to deal with due to insurmountable mathematical complexities associated with the noncommutability between spin operators involved in its Hamiltonian; thus, one usually has to either rely on the applicability of some simpler approximative method or perform rather extensive numerical calculations. To the best of our knowledge, the spin-1/2 Heisenberg model on the triangulated kagome lattice has been studied yet merely in terms of the linear Holstein–Primakoff spin-wave theory[29] and the variational mean-field-like treatment.[30] Both the aforementioned methods have, however, obvious insufficiencies. The former method based on the spin-wave approximation is applicable only if the ratio between both interaction parameters is from the interval $1 \leq |J_{aa}/J_{ab}| \leq 3$; i.e., the frustrating antiferromagnetic intratrimer interaction J_{aa} might not be much too stronger than the ferromagnetic one, J_{ab}. On the other hand, the latter method based on the variational mean-field-like treatment is asymptotically exact in the $|J_{ab}/J_{aa}| \rightarrow 0$ limit, but it fails to predict the disordered ground state for any finite ratio $|J_{ab}/J_{aa}|$.[26]

In view of this, the present work aims to suggest and exactly solve the spin-1/2 Ising-Heisenberg model on the triangulated kagome lattice by establishing a precise mapping relationship with the corresponding spin-1/2 Ising model on the simple kagome lattice. Within the framework of the proposed Ising-Heisenberg model, the exchange interaction between the trimeric a sites is being treated as the *XXZ* Heisenberg interaction $J_{aa} = J_H(\Delta)$, while the exchange interaction between the trimeric a sites and monomeric b sites will be approximated by the Ising-type interaction $J_{ab} = J_I$. Even though this model also has a clear deficiency in that the monomer-trimer interaction is considered as the Ising-type interaction, it should be much more reliable in describing the

frustrated magnetism of $Cu_9X_2(cpa)_6$ compounds as it correctly takes into account quantum fluctuations between the trimeric a sites. In addition, it is also quite plausible to argue that the monomeric b sites are in the frustrated regime completely free to flip without any energy cost and hence, the Ising character of the monomer-trimer interaction might be regarded as at least a quite reasonable first-order approximation.

The rest of this paper is organized as follows: In Sec. II, we provide a detailed description of the model under investigation and then, basic steps of our exact analytical treatment are explained. The most interesting results are presented and discussed in detail in Sec. III, where a particular emphasis is laid on a physical understanding of the ground-state and finite-temperature phase diagrams, as well as the temperature dependences of several thermodynamical quantities. Some conclusions are finally drawn in Sec. IV.

II. MODEL AND ITS EXACT SOLUTION

Let us define the spin-1/2 Ising-Heisenberg model on the triangulated kagome lattice (Fig. 1), which resembles a rather curious magnetic structure discovered in the series of polymeric coordination compounds $Cu_9X_2(cpa)_6$.[21] The magnetic properties of this series are captured to the lattice positions of Cu^{2+} ions, which are situated at two inequivalent lattice positions previously referred to as the trimeric a sites (empty circles) and the monomeric b sites (full circles). Let us now assign the *Heisenberg spin* $S=1/2$ to each trimeric a site and the *Ising spin* $\mu=1/2$ to each monomeric b site.[31] In this way, the exchange interaction J_{aa} between Cu^{2+} ions located at the nearest-neighbor trimeric sites will be treated as the Heisenberg interaction $J_H(\Delta)$, while the exchange interaction J_{ab} between two Cu^{2+} ions located at the nearest-neighbor trimeric and monomeric sites will be treated as the Ising interaction J_I. The total Hamiltonian of the model under investigation then reads

$$\hat{\mathcal{H}} = -J_H \sum_{(i,j)} [\Delta(\hat{S}_i^x \hat{S}_j^x + \hat{S}_i^y \hat{S}_j^y) + \hat{S}_i^z \hat{S}_j^z] - J_I \sum_{(k,l)} \hat{S}_k^z \hat{\mu}_l^z, \quad (1)$$

where the first summation is carried out over all pairs of the nearest-neighbor Heisenberg spins and the second summation extends over all pairs of the nearest-neighbor Heisenberg and Ising spins, respectively. The spin operators $\hat{S}_i^\alpha$ ($\alpha = x, y, z$) and $\hat{\mu}_l^z$ denote spatial components of the usual spin-1/2 operator and the parameter Δ will allow us to control the exchange anisotropy in the anisotropic *XXZ* Heisenberg interaction and to obtain the Ising model as a special limiting case for $\Delta = 0$. Finally, the total number of the Ising spins (b sites) is set to N, which implies that the total number of all spins (lattice sites) is $N_T = 3N$.

For further convenience, total Hamiltonian (1) can be written as a sum over six-spin cluster Hamiltonians $\hat{\mathcal{H}} = \Sigma_k \hat{\mathcal{H}}_k$; whereas each cluster Hamiltonian $\hat{\mathcal{H}}_k$ involves all the interaction terms associated with three Heisenberg spins from the kth trimer (see Fig. 1),

$$\hat{\mathcal{H}}_k = -J_H[\Delta(\hat{S}_{k1}^x \hat{S}_{k2}^x + \hat{S}_{k1}^y \hat{S}_{k2}^y) + \hat{S}_{k1}^z \hat{S}_{k2}^z] - J_H[\Delta(\hat{S}_{k2}^x \hat{S}_{k3}^x + \hat{S}_{k2}^y \hat{S}_{k3}^y) + \hat{S}_{k2}^z \hat{S}_{k3}^z] - J_H[\Delta(\hat{S}_{k3}^x \hat{S}_{k1}^x + \hat{S}_{k3}^y \hat{S}_{k1}^y) + \hat{S}_{k3}^z \hat{S}_{k1}^z] - \hat{S}_{k1}^z(h_{k1} + h_{k2}) - \hat{S}_{k2}^z(h_{k2} + h_{k3}) - \hat{S}_{k3}^z(h_{k3} + h_{k1}), \quad (2)$$

where $h_{ki} = J_I \hat{\mu}_{ki}^z$. Obviously, six-spin cluster Hamiltonian (2) might be regarded as the Hamiltonian of the kth Heisenberg trimer placed in some generally nonuniform magnetic field produced by three surrounding Ising spins. By taking into account the commutability between different cluster Hamiltonians $[\hat{\mathcal{H}}_i, \hat{\mathcal{H}}_j] = 0$ valid for each $i \neq j$, the partition function of the spin-1/2 Ising-Heisenberg model on the triangulated kagome lattice can be partially factorized into the product of cluster partition functions $\mathcal{Z}_k$,

$$\mathcal{Z} = \sum_{\{\mu_i\}} \prod_{k=1}^{2N/3} \text{Tr}_k \exp(-\beta \hat{\mathcal{H}}_k) = \sum_{\{\mu_i\}} \prod_{k=1}^{2N/3} \mathcal{Z}_k. \quad (3)$$

Above, the summation $\Sigma_{\{\mu_i\}}$ runs over all possible spin configurations of the Ising spins and the symbol Tr_k stands for a trace over spin degrees of freedom of the kth Heisenberg trimer. To proceed further with the calculation, it is very convenient to accomplish an exact analytical diagonalization of cluster Hamiltonian (2) in a particular Hilbert subspace corresponding to the kth Heisenberg trimer. If doing so, the resulting cluster partition function $\mathcal{Z}_k$ will depend on just three Ising spins μ_{k1}, μ_{k2}, and μ_{k3}, which are included in the parameters h_{k1}, h_{k2}, and h_{k3} determining the "local magnetic fields" acting on the Heisenberg spins. Moreover, the explicit mathematical form of the cluster partition function $\mathcal{Z}_k$ immediately implies a possibility of performing the generalized star-triangle mapping transformation[32,33]

$$\mathcal{Z}_k = 2 \exp\left(\frac{3\beta J_H}{4}\right) \cosh[\beta J_I(\mu_{k1}^z + \mu_{k2}^z + \mu_{k3}^z)]$$

$$+ \exp\left[-\frac{\beta J_H}{4} + \frac{\beta J_I}{3}(\mu_{k1}^z + \mu_{k2}^z + \mu_{k3}^z)\right]$$

$$\times \sum_{n=0}^{2} \exp\left[-2\beta \, \text{sgn}(Q_+)\sqrt{P} \cos\left(\Phi_+ + \frac{2\pi n}{3}\right)\right]$$

$$+ \exp\left[-\frac{\beta J_H}{4} - \frac{\beta J_I}{3}(\mu_{k1}^z + \mu_{k2}^z + \mu_{k3}^z)\right]$$

$$\times \sum_{n=0}^{2} \exp\left[-2\beta \, \text{sgn}(Q_-)\sqrt{P} \cos\left(\Phi_- + \frac{2\pi n}{3}\right)\right]$$

$$= A \exp[\beta J_{\text{kag}}^{\text{eff}}(\mu_{k1}^z \mu_{k2}^z + \mu_{k2}^z \mu_{k3}^z + \mu_{k3}^z \mu_{k1}^z)], \quad (4)$$

where $\beta = 1/(k_B T)$, k_B is Boltzmann's constant, T is the absolute temperature, and the parameters P, $Q_\pm$, and $\Phi_\pm$ are defined as follows:

$$P = \left(\frac{J_I}{3}\right)^2 \left[\frac{3}{4} - (\mu_{k1}^z \mu_{k2}^z + \mu_{k2}^z \mu_{k3}^z + \mu_{k3}^z \mu_{k1}^z)\right] + \left(\frac{J_H \Delta}{2}\right)^2,$$

$$(5)$$

$$Q_\pm = \pm \frac{1}{2}\left(\frac{J_I}{3}\right)^3 (\mu_{k1}^z + \mu_{k2}^z + \mu_{k3}^z - 12\mu_{k1}^z\mu_{k2}^z\mu_{k3}^z) - \left(\frac{J_H\Delta}{2}\right)^3, \tag{6}$$

$$\Phi_\pm = \frac{1}{3}\arctan\left(\frac{\sqrt{P^3 - Q_\pm^2}}{Q_\pm}\right). \tag{7}$$

From here onward, our procedure closely follows the approach developed by Zheng and Sun[25] that relates an exact solution of the spin-1/2 Ising model on the triangulated kagome lattice to an exact solution of the corresponding spin-1/2 Ising model on the simple kagome lattice.[25] As a matter of fact, star-triangle transformation (4) effectively removes all the interaction terms associated with the *k*th Heisenberg trimer and substitutes them with the effective interaction $J_{\mathrm{kag}}^{\mathrm{eff}}$ between three enclosing Ising spins μ_{k1}, μ_{k2}, and μ_{k3}. Of course, mapping transformation (4) must hold for any available spin configuration of three enclosing Ising spins and this self-consistency condition unambiguously determines so far not specified mapping parameters A and $\beta J_{\mathrm{kag}}^{\mathrm{eff}}$,

$$A = (V_1 V_2^3)^{1/4} \quad \text{and} \quad \beta J_{\mathrm{kag}}^{\mathrm{eff}} = \ln(V_1/V_2). \tag{8}$$

The functions V_1 and V_2 entering into the effective mapping parameters A and $\beta J_{\mathrm{kag}}^{\mathrm{eff}}$ are actually two independent expressions for cluster partition function (4) to be obtained by considering all eight possible spin configurations available to three enclosing Ising spins,

$$V_1 = 2\exp\left(\frac{3\beta J_H}{4}\right)\cosh\left(\frac{3\beta J_I}{2}\right) + 2\exp\left(-\frac{\beta J_H}{4}\right)\cosh\left(\frac{\beta J_I}{2}\right)$$
$$\times\left[\exp(\beta J_H\Delta) + 2\exp\left(-\frac{\beta J_H\Delta}{2}\right)\right], \tag{9}$$

$$V_2 = 2\exp\left(\frac{3\beta J_H}{4}\right)\cosh\left(\frac{\beta J_I}{2}\right) + \exp\left(-\frac{\beta J_H}{4} + \frac{\beta J_I}{6}\right)$$
$$\times\sum_{n=0}^{2}\exp\left[-2\beta\,\mathrm{sgn}(q_+)\sqrt{p}\,\cos\left(\phi_+ + \frac{2\pi n}{3}\right)\right]$$
$$+ \exp\left(-\frac{\beta J_H}{4} - \frac{\beta J_I}{6}\right)\sum_{n=0}^{2}\exp\left[-2\beta\,\mathrm{sgn}(q_-)\sqrt{p}\right.$$
$$\times\cos\left(\phi_- + \frac{2\pi n}{3}\right)\bigg], \tag{10}$$

and the parameters p, $q_\pm$, and $\phi_\pm$ are defined as follows:

$$p = \left(\frac{J_I}{3}\right)^2 + \left(\frac{J_H\Delta}{2}\right)^2, \tag{11}$$

$$q_\pm = \pm\left(\frac{J_I}{3}\right)^3 - \left(\frac{J_H\Delta}{2}\right)^3, \tag{12}$$

$$\phi_\pm = \frac{1}{3}\arctan\left(\frac{\sqrt{p^3 - q_\pm^2}}{q_\pm}\right). \tag{13}$$

By substituting mapping transformation (4) into the relevant expression for partition function (3), one establishes a simple mapping relationship between the partition function of the spin-1/2 Ising-Heisenberg model on the triangulated kagome lattice and the partition function of the corresponding spin-1/2 Ising model on the kagome lattice,

$$\mathcal{Z}(\beta, J_H, \Delta, J_I) = A^{2N/3}\mathcal{Z}_{\mathrm{kag}}(\beta J_{\mathrm{kag}}^{\mathrm{eff}}). \tag{14}$$

This relation actually completes our exact calculation of the partition function as the corresponding exact result for the partition function of the spin-1/2 Ising model on the kagome lattice is well known.[34–36] At this stage, exact results for other thermodynamic quantities follow straightforwardly. The Helmholtz free energy of the spin-1/2 Ising-Heisenberg model on the triangulated kagome lattice may be connected to the Helmholtz free energy of the corresponding spin-1/2 Ising model on the kagome lattice ($\mathcal{F}_{\mathrm{kag}} = -\beta^{-1}\ln\mathcal{Z}_{\mathrm{kag}}$) through the relation

$$\mathcal{F} = \mathcal{F}_{\mathrm{kag}} - 2N\beta^{-1}\ln A/3. \tag{15}$$

The connection between the internal energy of spin-1/2 Ising-Heisenberg model on the triangulated kagome lattice and that one of the corresponding spin-1/2 Ising model on the kagome lattice can readily be obtained by differentiating the logarithm of Eq. (14) with respect to the inverse temperature β yielding

$$\mathcal{U} = -\frac{\partial\ln\mathcal{Z}}{\partial\beta} = -\frac{2N}{3}\frac{\partial\ln A}{\partial\beta} - \frac{\partial\ln\mathcal{Z}_{\mathrm{kag}}}{\partial(\beta J_{\mathrm{kag}}^{\mathrm{eff}})}\frac{\partial(\beta J_{\mathrm{kag}}^{\mathrm{eff}})}{\partial\beta}$$
$$= \frac{W_1}{V_1}\left(\frac{\mathcal{U}_{\mathrm{kag}}}{J_{\mathrm{kag}}^{\mathrm{eff}}} - \frac{N}{6}\right) - \frac{W_2}{V_2}\left(\frac{\mathcal{U}_{\mathrm{kag}}}{J_{\mathrm{kag}}^{\mathrm{eff}}} + \frac{N}{2}\right). \tag{16}$$

Note that the exact result for the internal energy of the spin-1/2 Ising model on the kagome lattice is well known (see, for instance, Ref. 36) and thus, our exact calculation is essentially completed by introducing the parameters W_1 and W_2 that denote inverse temperature derivatives of the functions V_1 and V_2 given by Eqs. (9) and (10),

$$W_1 = \frac{\partial V_1}{\partial\beta}$$
$$= \frac{3}{2}\exp\left(\frac{3\beta J_H}{4}\right)\left[J_H\cosh\left(\frac{3\beta J_I}{2}\right) + 2J_I\sinh\left(\frac{3\beta J_I}{2}\right)\right]$$
$$+ \exp\left(-\frac{\beta J_H}{4} + \beta J_H\Delta\right)\left[\left(2J_H\Delta - \frac{J_H}{2}\right)\cosh\left(\frac{\beta J_I}{2}\right)\right.$$
$$+ J_I\sinh\left(\frac{\beta J_I}{2}\right)\bigg] - \exp\left(-\frac{\beta J_H}{4} - \frac{\beta J_H\Delta}{2}\right)$$
$$\times\left[(2J_H\Delta + J_H)\cosh\left(\frac{\beta J_I}{2}\right) - 2J_I\sinh\left(\frac{\beta J_I}{2}\right)\right], \tag{17}$$

$$W_2 = \frac{\partial V_2}{\partial \beta}$$

$$= \exp\left(\frac{3\beta J_H}{4}\right)\left[\frac{3}{2}J_H \cosh\left(\frac{\beta J_I}{2}\right) + J_I \sinh\left(\frac{\beta J_I}{2}\right)\right]$$

$$- \sum_{n=0}^{2}\left[\frac{J_H}{4} - \frac{J_I}{6} + 2\,\mathrm{sgn}(q_+)\sqrt{p}\,\cos\left(\phi_+ + \frac{2\pi n}{3}\right)\right]$$

$$\times \exp\left[-\frac{\beta J_H}{4} + \frac{\beta J_I}{6} - 2\beta\,\mathrm{sgn}(q_+)\right.$$

$$\left.\times \sqrt{p}\,\cos\left(\phi_+ + \frac{2\pi n}{3}\right)\right] - \sum_{n=0}^{2}\left[\frac{J_H}{4} + \frac{J_I}{6} + 2\,\mathrm{sgn}(q_-)\right.$$

$$\left.\times \sqrt{p}\,\cos\left(\phi_- + \frac{2\pi n}{3}\right)\right]\exp\left[-\frac{\beta J_H}{4} - \frac{\beta J_I}{6} - 2\beta\,\mathrm{sgn}(q_-)\right.$$

$$\left.\times \sqrt{p}\,\cos\left(\phi_- + \frac{2\pi n}{3}\right)\right]. \tag{18}$$

The entropy can be now easily calculated either from the basic thermodynamic relation between Helmholtz free energy and internal energy, $\mathcal{F} = \mathcal{U} - T\mathcal{S}$, or as a negative temperature derivative of free energy (15). Both procedures yield the following closed-form relation for the reduced entropy per one site of the original spin-1/2 Ising-Heisenberg model on the triangulated kagome lattice:

$$\frac{\mathcal{S}}{N_T k_B} = \frac{1}{3N}\ln \mathcal{Z}_{\mathrm{kag}} + \frac{2}{9}\ln A + \frac{\beta W_1}{3V_1}\left(\frac{\mathcal{U}_{\mathrm{kag}}}{N J_{\mathrm{kag}}^{\mathrm{eff}}} - \frac{1}{6}\right)$$

$$- \frac{\beta W_2}{3V_2}\left(\frac{\mathcal{U}_{\mathrm{kag}}}{N J_{\mathrm{kag}}^{\mathrm{eff}}} + \frac{1}{2}\right). \tag{19}$$

It is quite obvious from the above formula that the reduced entropy of the spin-1/2 Ising-Heisenberg model on the triangulated kagome lattice can be expressed in terms of the known exact results for the partition function[35] and internal energy[36] of the corresponding spin-1/2 Ising model on the kagome lattice. It is worthy to note, moreover, that the zero-field specific heat can also be simply obtained as a temperature derivative of internal energy (16), but the final expression is too cumbersome to write down here explicitly.

III. RESULTS AND DISCUSSION

Before proceeding to a discussion of the most interesting results, it is quite useful to realize that all final results derived in Sec. II are invariant under the transformation $J_I \rightarrow -J_I$. For this reason, it is very convenient to set the absolute value of the Ising interaction $|J_I|$ as the energy unit and to define two dimensionless parameters $k_B T/|J_I|$ and $J_H/|J_I|$, reducing the number of free parameters. The former dimensionless parameter is then proportional to the relative size of the temperature, while the latter one determines the relative strength of the intratrimer Heisenberg interaction J_H with respect to the monomer-trimer Ising interaction J_I.

First, let us take a closer look at the ground-state behavior. It is quite evident that the spin-1/2 Ising-Heisenberg model
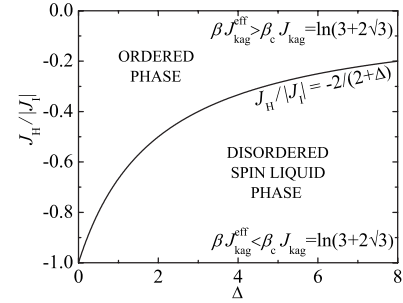

FIG. 2. Ground-state phase diagram in the $\Delta - J_H/|J_I|$ plane separating the spontaneously ordered and disordered phases.

on the triangulated kagome lattice exhibits spontaneous long-range ordering if and only if the corresponding spin-1/2 Ising model on the simple kagome lattice is spontaneously long-range ordered as well. Accordingly, the ground-state phase diagram can readily be obtained from a comparison of the effective interaction parameter $\beta J_{\mathrm{kag}}^{\mathrm{eff}}$ given by Eq. (8) with the critical point of the spin-1/2 Ising model on the kagome lattice $\beta_c J_{\mathrm{kag}} = \ln(3 + 2\sqrt{3})$ $[\beta_c = 1/(k_B T_c)$, where T_c is the critical temperature].[34] In consequence of that, the ground state is spontaneously long-range ordered if $\beta J_{\mathrm{kag}}^{\mathrm{eff}} > \ln(3 + 2\sqrt{3})$, while it becomes disordered spin liquid state as long as $\beta J_{\mathrm{kag}}^{\mathrm{eff}} < \ln(3 + 2\sqrt{3})$. The phase boundary between ordered and disordered ground states, which follows from the zero-temperature limit of mapping parameter (8), is shown in Fig. 2 and can be expressed through the following analytical condition:

$$J_H/|J_I| = -2/(2 + \Delta). \tag{20}$$

It can be easily understood that the disordered spin liquid state appears as a result of geometric frustration, which comes into play provided that there is a sufficiently strong antiferromagnetic Heisenberg interaction. Indeed, the ground state is a simple ferromagnetic or ferrimagnetic spin arrangement for any $J_H/|J_I|$ greater than boundary value (20) depending on whether $J_I > 0$ or $J_I < 0$; otherwise it becomes the disordered spin liquid state. Apparently, the greater the anisotropy constant Δ is, the weaker is the antiferromagnetic Heisenberg interaction needed to destroy the spontaneous long-range ordering.

Now, let us make a few remarks on the nature of possible ground states. The ferromagnetic as well as ferrimagnetic ordered states can be characterized through the same classical spin ordering as previously described by the analysis of the spin-1/2 Ising model on the triangulated kagome lattice.[26] As far as the disordered spin liquid state is concerned, however, there is a fundamental difference between the disordered ground state of the spin-1/2 Ising-Heisenberg model with any $\Delta \neq 0$ and its semiclassical Ising limit $\Delta = 0$. As a matter of fact, considering the frustrated regime $J_H/|J_I| < -1$ and setting $\Delta = 0$ into Eq. (8) gives the zero effective exchange coupling $\beta J_{\mathrm{kag}}^{\mathrm{eff}} = 0$, which means that the disordered ground state of the spin-1/2 Ising model on the triangulated kagome lattice is equivalent to an ensemble of noninteracting spins, or equivalently, to a spin system at infinite temperature. This implies that the Ising spins at the mono-

meric b sites are completely free to flip and the ground-state degeneracy of the disordered spin liquid state can be straight-forwardly counted by following the argument of Loh *et al.*[26] The residual entropy per spin is accordingly $S_0/N_T k_B = \frac{1}{9}\ln 72 = 0.4752$, since each trimeric unit has precisely three different lowest-energy states for each possible spin configuration of its three surrounding monomeric spins and the basic unit cell contains two trimeric units and three monomeric spins.

Contrary to this, effective exchange coupling (8) that corresponds to the spin-1/2 Ising-Heisenberg model on the triangulated kagome lattice with any $\Delta \neq 0$ is equal to $\beta J_{\text{kag}}^{\text{eff}} = \ln 2$ in the disordered region. Even though this value is smaller than the critical value $\beta_c J_{\text{kag}}$ and the spin system must be consequently disordered, its positive and nonzero value indicates a ferromagnetic character of short-range correlations between the monomeric Ising spins. It actually turns out that the lowest-energy state of each Heisenberg trimer is twofold degenerate if all three surrounding Ising spins are aligned alike (all three Ising spins point either "up" or "down"), while there is just one lowest-energy state from the ground-state manifold provided that two from three Ising spins are aligned alike and the third spin points in the opposite direction (remember that the lowest-energy state of the trimeric unit is threefold degenerate irrespective of the spin configuration of monomeric spins within the Ising model). With regard to this, the residual entropy of the disordered spin liquid phase is significantly lower for the quantum Ising-Heisenberg model than for its semiclassical Ising limit, $S_0/N_T k_B = 0.2806$ and 0.4752, respectively, which implies that quantum fluctuations partially lift the macroscopic degeneracy of the ground-state manifold. The most surprising finding stemming from our study is that the zero-point entropy of the spin-1/2 Ising-Heisenberg model is the same for arbitrary but nonzero anisotropy Δ and this observation suggests that the semiclassical Ising limit represents a very special limiting case of the model under consideration.

To provide an independent check of the aforementioned scenario, we depict in Fig. 3 temperature variations of the effective interaction $\beta J_{\text{kag}}^{\text{eff}}$ for several values of the ratio $J_H/|J_I|$ and two different values of the anisotropy constant $\Delta = 0$ and 1. It should be mentioned that the particular case of $\Delta = 1$ qualitatively resembles temperature dependences of the mapping parameter $\beta J_{\text{kag}}^{\text{eff}}$ for the Ising-Heisenberg model with any $\Delta \neq 0$. The considered model system is spontaneously long-range ordered below certain critical temperature if and only if the effective interaction parameter $\beta J_{\text{kag}}^{\text{eff}}$ is greater than the critical value $\beta_c J_{\text{kag}} = \ln(3+2\sqrt{3})$, shown in Fig. 3 as a broken line. In agreement with the aforedescribed ground-state analysis, the effective interaction starts from zero, then gradually increases to some local maximum before it finally goes to zero with increasing temperature whenever $\Delta = 0$ and $J_H/|J_I| < -1$. On the other hand, the effective interaction generally starts from the value $\ln 2$, then exhibits a temperature-induced local maximum before it finally tends to zero whenever $\Delta \neq 0$ and $J_H/|J_I| < -2/(2+\Delta)$. It is also quite evident from Fig. 3 that the spin system remains disordered over the whole temperature range for any $J_H/|J_I| < -2/(2+\Delta)$, since the effective interaction $\beta J_{\text{kag}}^{\text{eff}}$ never crosses the critical value $\beta_c J_{\text{kag}}$ that is needed to invoke a spontaneous
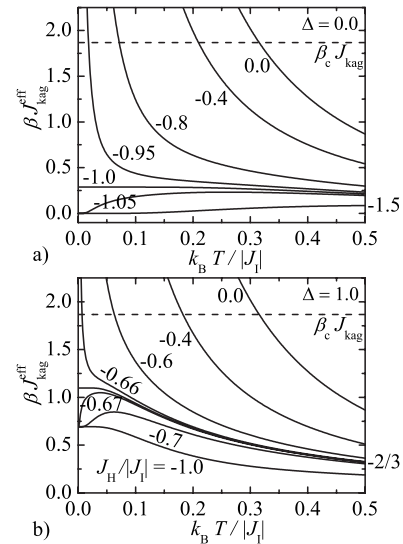

FIG. 3. Temperature dependences of the effective interaction $\beta J_{\text{kag}}^{\text{eff}}$ for several values of the ratio $J_H/|J_I|$ and two different anisotropy constants: (a) $\Delta = 0$; (b) $\Delta = 1$. The broken line shows the critical point $\beta_c J_{\text{kag}} = \ln(3+2\sqrt{3})$ of the corresponding spin-1/2 Ising model on the kagome lattice.

ordering. This observation would suggest that the Ising-Heisenberg model in question cannot exhibit a temperature-induced re-entrant phase transition from the disordered toward the spontaneously ordered phase regardless of whether $\Delta = 0$ or $\Delta \neq 0$.

At this point, let us proceed to a discussion of the finite-temperature phase diagram. The critical temperature of the spin-1/2 Ising-Heisenberg model on the triangulated kagome lattice can easily be calculated from the critical condition $\beta_c J_{\text{kag}}^{\text{eff}} = \ln(3+2\sqrt{3})$, which ensures that the corresponding spin-1/2 Ising model on the kagome lattice is precisely at the critical point. Note that this critical condition is essentially equivalent to a graphical solution that finds points of intersection between the temperature dependence of the effective interaction $\beta J_{\text{kag}}^{\text{eff}}$ and the critical point $\beta_c J_{\text{kag}} = \ln(3+2\sqrt{3})$ of the spin-1/2 Ising model on the kagome lattice (see Fig. 3). The dependence of the dimensionless critical temperature $k_B T_c/|J_I|$ on the ratio $J_H/|J_I|$ is displayed in Fig. 4 for several values of the anisotropy parameter Δ. As one can see, the critical temperature monotonically decreases with decreasing $J_H/|J_I|$ ratio until it vanishes at ground-state phase boundary (20) whenever the easy-axis exchange anisotropies $\Delta < 1$ are assumed. By contrast, the interesting nonmonotonic dependence of the critical temperature may be observed for the easy-plane anisotropies $\Delta > 1$ presumably due to a competition between the easy-axis Ising interaction J_I and the easy-plane Heisenberg interaction $J_H(\Delta)$ before the critical line finally tends to zero-temperature limit consistent with ground-state boundary (20). Several limiting cases of the model under investigation can be checked. First, the critical line of the spin-1/2 Ising model on the triangulated kagome lattice originally reported by Zheng and Sun[25] and later rederived by Loh *et al.*[26] is recovered on the assumption that $\Delta = 0$. By assuming $J_H/|J_I| = 0$, on the other hand, all critical lines meet at a common critical point,
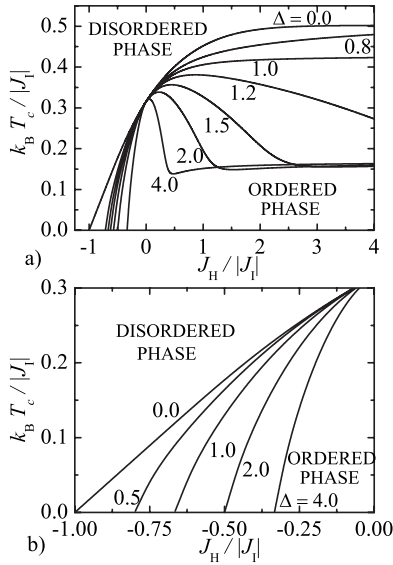
FIG. 4. The dimensionless critical temperature $k_B T_c / |J_I|$ as a function of the ratio $J_H / |J_I|$ for different values of the exchange anisotropy Δ. (b) shows a detail of the finite-temperature phase diagram, where the critical temperature tends toward the zero temperature.

$$\frac{k_B T_c}{|J_I|} = \frac{1}{2 \ln(\sqrt{3 + 2\sqrt{3}} + \sqrt{2 + 2\sqrt{3}})} \doteq 0.3154, \quad (21)$$

which is consistent with the critical temperature of the spin-1/2 Ising model on the decorated kagome lattice. It is also quite interesting to check the asymptotic behavior of the critical temperature achieved in the limit $J_H / |J_I| \to \infty$ that corresponds to the infinitely strong ferromagnetic Heisenberg interaction. If $\Delta < 1$, the critical temperature asymptotically reaches the value

$$\frac{k_B T_c}{|J_I|} = \frac{1}{\ln(2 + \sqrt{3} + \sqrt{6 + 4\sqrt{3}})} \doteq 0.5021, \quad (22)$$

while for $\Delta > 1$ it strikingly decreases down to one-third of this asymptotic value,

$$\frac{k_B T_c}{|J_I|} = \frac{1}{3 \ln(2 + \sqrt{3} + \sqrt{6 + 4\sqrt{3}})} \doteq 0.1673. \quad (23)$$

For the particular case $\Delta = 1$, the critical temperature of the spin-1/2 Ising-Heisenberg model on the triangulated kagome lattice acquires in the limit $J_H / |J_I| \to \infty$ the asymptotic value $k_B T_c / |J_I| \doteq 0.4285$.

Next, let us turn our attention to temperature dependences of some thermodynamic quantities. Figure 5 depicts temperature variations of the entropy calculated for several values of the ratio $J_H / |J_I|$ and two different values of the anisotropy $\Delta = 0$ and 1. As it can be clearly seen, the standard S-shaped dependence with a weak energylike singularity located at critical points of the order-disorder phase transitions, which are schematically shown in Fig. 5 as open circles, gradually shifts toward zero temperature upon strengthening of the antiferromagnetic Heisenberg interaction until the
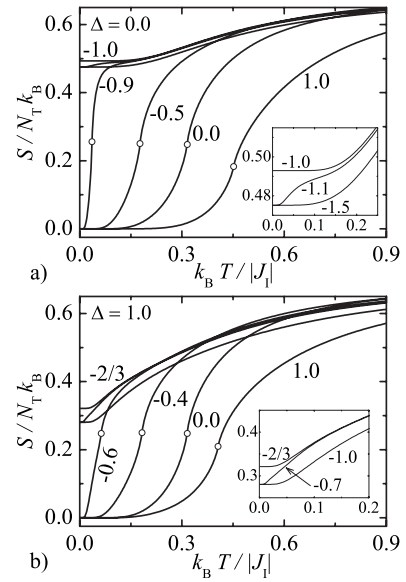

FIG. 5. Thermal variations of the entropy for different values of the ratio $J_H / |J_I|$, which are indicated by the numbers associated with each line, and two different values of the anisotropy constant: (a) $\Delta = 0$; (b) $\Delta = 1$. The inset shows the low-temperature behavior for special cases, where the entropy tends toward its residual values.

weak singularity completely disappears from the entropy dependence whenever $J_H / |J_I| < -2/(2 + \Delta)$. Under this circumstance, the displayed thermal dependences tend asymptotically toward the zero-point entropy $S_0 / N_T k_B = 0.2806$ or 0.4752 depending on whether $\Delta \neq 0$ or $\Delta = 0$, respectively. The low-temperature behavior of the entropy, which is for better clarity shown in the inset of Fig. 5, thus provides an independent confirmation of the macroscopic degeneracy that appears within the disordered spin liquid ground states.

Finally, let us conclude our analysis of thermodynamics by exploring the temperature dependences of the zero-field specific heat. For illustration, some typical thermal variations of the specific heat are plotted in Figs. 6 and 7 for several values of the ratio $J_H / |J_I|$ and two different values of the exchange anisotropy $\Delta = 0$ and 1. The upper panels in both
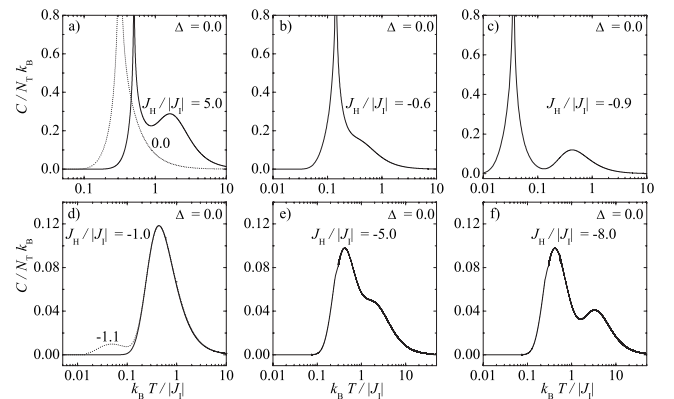

FIG. 6. Some typical temperature dependences of the zero-field specific heat of the spin-1/2 Ising model on the triangulated kagome lattice with $\Delta = 0$, which can be obtained by changing the strength of the interaction ratio $J_H / |J_I|$.
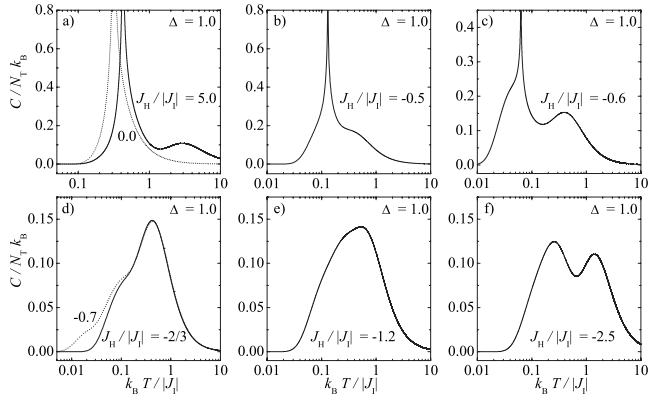
FIG. 7. Some typical temperature dependences of the zero-field specific heat of the spin-1/2 Ising-Heisenberg model on the triangulated kagome lattice with $\Delta = 1$, which can be obtained by changing the strength of the interaction ratio $J_H/|J_I|$.

figures depict the particular cases with the spontaneously long-range ordered ground state, whereas the lower panels show the particular cases with the disordered spin liquid ground state. In accordance with the above statement, all temperature dependences of the heat capacity shown in both upper panels display a logarithmic singularity from the standard Ising universality class, which is associated with the continuous (second-order) phase transition between the spontaneously ordered and disordered phases. Even though the specific-heat curves displayed in Figs. 6 and 7 have several common features, there are nevertheless a few important differences. In both cases, the marked round maximum is superimposed on the high-temperature tail of the specific-heat singularity by considering a strong ferromagnetic intratrimer interaction $J_H/|J_I| \gg 1$ [see Figs. 6(a) and 7(a)]. However, it can be also clearly seen that this round maximum is much more pronounced in the Ising model with $\Delta = 0$ than in the Ising-Heisenberg model with $\Delta = 1$. It is worthwhile to remark, moreover, that the round maximum in the high-temperature tail of the specific heat can be also observed when taking into account the antiferromagnetic intratrimer interaction $J_H/|J_I| < 0$ [see Figs. 6(b), 6(c), 7(b), and 7(c)], but in this particular case, the robust hump develops only if the ratio $J_H/|J_I|$ is close enough to boundary value (20). In this parameter space, the most important difference between the specific-heat curves of the Ising and Ising-Heisenberg models lies in an appearance of the additional marked shoulder, which appears in the low-temperature tail of the heat capacity in the latter model only [Fig. 7(c)], whereas this feature is obviously missing in the relevant dependence of the former model [Fig. 6(c)].

Last but not the least, let us comment on temperature dependences of the specific heat by considering some typical cases that correspond to a spin system with the disordered spin liquid ground state (the lower panels in Figs. 6 and 7). Apparently, the temperature dependence with a single maximum is obtained by selecting the ratio $J_H/|J_I|$ exactly from ground-state boundary (20) between the spontaneously ordered and disordered phases [see Figs. 6(d) and 7(d)]. Note that this maximum is nevertheless much less symmetric for the Ising-Heisenberg model [Fig. 7(d)] than for its Ising

counterpart [Fig. 6(d)], while both models exhibit a quite similar uprise of the additional low-temperature shoulder upon a consecutive slight decrease in the ratio $J_H/|J_I|$. As evidenced by Fig. 7(e), the specific heat of the Ising-Heisenberg model gradually looses its irregular shape upon further decrease in the interaction parameter $J_H/|J_I|$. It is noteworthy, moreover, that the specific-heat curve with two marked rounded maxima appear by assuming a sufficiently strong antiferromagnetic intratrimer interaction $J_H/|J_I| \ll -1$ [Figs. 6(f) and 7(f)]; whereas the more negative the ratio $J_H/|J_I|$ is, the more evident the double-peak structure of the zero-field specific-heat curve is. However, it should be also pointed out that the temperature dependence with the double-peak specific heat emerges in the Ising-Heisenberg model with $\Delta = 1$ for much smaller geometric frustration (i.e., less negative ratio $J_H/|J_I|$) than for the Ising model with $\Delta = 0$. Notwithstanding this observation, the specific-heat curves with two well-separated maxima might be expected for the series of polymeric coordination compounds $Cu_9X_2(cpa)_6$ for which a rough estimate of the ratio $|J_{aa}/J_{ab}| \approx 40$ has been made according to the experimentally measured susceptibility data.[23]

IV. CONCLUDING REMARKS

The present paper provides a survey of exact analytical results for the spin-1/2 Ising-Heisenberg model on the triangulated kagome (triangles-in-triangles) lattice, which has been proposed in order to shed light on a frustrated magnetism of the series of $Cu_9X_2(cpa)_6$ polymeric coordination compounds. The model under investigation has exactly been solved with the help of generalized star-triangle transformation that establishes a precise mapping relationship to the corresponding spin-1/2 Ising model on the kagome lattice. Exact results for the ground-state and finite-temperature phase diagrams, as well as several thermodynamic quantities such as the Helmholtz free energy, internal energy, entropy, and specific heat, have been derived and discussed in detail.

Even though a theoretical description based on the hybrid Ising-Heisenberg model may not be fully realistic for true magnetic materials from the family of copper-based coordination compounds (Heisenberg model would be, of course, more adequate), it is quite reasonable to expect that the presented exact results illustrate many important features of the series of three isostructural compounds $Cu_9X_2(cpa)_6$. It is really plausible to argue that the suggested model correctly takes into account quantum effects closely connected with the stronger intratrimer Heisenberg interaction J_H, whereas the Ising character of the weaker monomer-trimer interaction J_I might be regarded as at least rather reasonable first-order approximation. This approximation should be altogether acceptable especially in the highly frustrated region $J_H/|J_I| \ll -2/(2+\Delta)$, where the "Ising" spins located at the monomeric sites are completely free to flip without any energy cost owing to a strong geometric frustration produced by the trimeric "Heisenberg" spins. From this perspective, it is quite tempting to conjecture that the zero-field specific heat of $Cu_9X_2(cpa)_6$ compounds should exhibit a notable temperature dependence with two outstanding round maxima, which

are well separated from each other because the antiferromagnetic intratrimer interaction is roughly 2 orders of magnitude stronger than the ferromagnetic monomer-trimer interaction.

In agreement with our expectations, it also has been demonstrated that quantum fluctuations introduced through the nonzero exchange anisotropy Δ help to destroy spontaneous (ferromagnetic or ferrimagnetic) long-range ordering. As a matter of fact, it can be readily understood from Eq. (20) that the increase in the anisotropy parameter Δ suppresses the strength of the antiferromagnetic intratrimer interaction that is needed to prevent spontaneous ordering. However, the most surprising finding to emerge from the present study closely relates to a substantial decline in the residual entropy of disordered spin liquid state, which appears on the assumption that there is an arbitrary but nonzero exchange anisotropy Δ. It actually turns out that the quantum fluctuations partially lift a rather high macroscopic degeneracy of the disordered spin liquid state and consequently, the zero-point entropy of the quantum Ising-Heisenberg model $S_0/N_T k_B = 0.2806$ is for any $\Delta \neq 0$ significantly lower than the zero-point entropy of the semiclassical Ising model $S_0/N_T k_B = 0.4752$ achieved in the limiting case $\Delta = 0$. From this point of view, another interesting question arises as to whether or not the residual entropy of the spin-1/2 Heisenberg model on the triangulated kagome lattice will be completely removed by the order-from-disorder mechanism[37] when accounting for the Heisenberg character of the monomer-trimer interaction as well. In order to clarify this unresolved issue, it is necessary to perform a rather extensive exact numerical diagonalization of the full Heisenberg Hamiltonian, or, alternatively, it would be also possible to use the exact solution of the Ising-Heisenberg model as a starting point of more general perturbative treatment.

Shortly after our paper was submitted for publication, Yao *et al.*[38] completed a similar work dealing with the spin-1/2 Ising-Heisenberg model on the triangulated kagome lattice. The main difference between our procedure and the one of Yao *et al.*[38] lies in the way of calculating the energy spectrum of Heisenberg trimer and its three enclosing Ising spins. In our procedure, we first performed an exact diagonalization of the Heisenberg trimer in some generally nonuniform local field produced by three surrounding Ising spins and then, we considered two symmetry-distinct configurations of the enclosing Ising spins in order to establish a precise mapping relationship with the corresponding spin-1/2 Ising model. In the procedure developed by Yao *et al.*,[38] the authors first consider two symmetry-distinct configurations of the enclosing Ising spins and then, they diagonalize the Heisenberg trimer for both symmetry-distinct configurations of the surrounding Ising spins. In such way, they were able to avoid rather cumbersome expressions for the roots of cubic equations, which otherwise occur when diagonalizing the Heisenberg trimer in some generally nonuniform local magnetic field. Despite this difference, both procedures turn out to be completely equivalent as it could be easily checked from a comparison of the effective mapping parameters calculated from our Eqs. (8)–(13) and Eqs. (7), (8), (13), and (14) of Yao *et al.*[38] Exact results presented in both papers for the ground-state and finite-temperature phase diagrams, Helmholtz free energy, internal energy and entropy are consequently in good accordance.

*jozef.strecka@upjs.sk, jozkos@pobox.sk; http://158.197.33.91/~strecka

[1] G. Misguich and C. Lhuillier, in *Frustrated Spin Systems*, edited by H. T. Diep (World Scientific, Singapore, 2004).

[2] J. Richter, J. Schulenburg, and A. Honecker, in *Quantum Magnetism*, Lecture Notes in Physics Vol. 645, edited by U. Schollwöck, J. Richter, D. J. J. Farnell, and R. F. Bishop (Springer, Berlin, 2004).

[3] A. Honecker, J. Schulenburg, and J. Richter, J. Phys.: Condens. Matter **16**, S749 (2004).

[4] C. Lhuillier and G. Misguich, Lect. Notes Phys. **595**, 161 (2002); C. Lhuillier, arXiv:cond-mat/0502464 (unpublished).

[5] S. Miyashita, J. Phys. Soc. Jpn. **55**, 3605 (1986); H. Nishimori and S. Miyashita, *ibid.* **55**, 4448 (1986); D. A. Huse and V. Elser, Phys. Rev. Lett. **60**, 2531 (1988); H. Nishimori and H. Nakanishi, J. Phys. Soc. Jpn. **57**, 626 (1988); A. V. Chubokov and D. I. Golosov, J. Phys.: Condens. Matter **3**, 69 (1991); B. Bernu, C. Lhuillier, and L. Pierre, Phys. Rev. Lett. **69**, 2590 (1992); P. W. Leung and K. J. Runge, Phys. Rev. B **47**, 5861 (1993); B. Bernu, P. Lecheminant, C. Lhuillier, and L. Pierre,

Phys. Scr. **t49a**, 192 (1993); B. Bernu, P. Lecheminant, C. Lhuillier, and L. Pierre, Phys. Rev. B **50**, 10048 (1994); L. Capriotti, A. E. Trumper, and S. Sorella, Phys. Rev. Lett. **82**, 3899 (1999); A. Honecker, J. Phys.: Condens. Matter **11**, 4697 (1999); C. Lhuillier, P. Sindzingre, and J. B. Fouet, Can. J. Phys. **79**, 1525 (2001).

[6] V. Elser, Phys. Rev. Lett. **62**, 2405 (1989); C. Zeng and V. Elser, Phys. Rev. B **42**, 8436 (1990); S. Sachdev, *ibid.* **45**, 12377 (1992); J. T. Chalker and J. F. G. Eastmond, *ibid.* **46**, 14201 (1992); R. R. P. Singh and D. A. Huse, Phys. Rev. Lett. **68**, 1766 (1992); P. W. Leung and V. Elser, Phys. Rev. B **47**, 5459 (1993); N. Elstner and A. P. Young, Phys. Rev. B **50**, 6871 (1994); C. Zeng and V. Elser, Phys. Rev. B **51**, 8318 (1995); P. Lecheminant, B. Bernu, C. Lhuillier, L. Pierre, and P. Sindzingre, *ibid.* **56**, 2521 (1997); Ch. Waldtmann, H.-U. Everts, B. Bernu, C. Lhuillier, P. Sindzingre, P. Lecheminant, and L. Pierre, Eur. Phys. J. B **2**, 501 (1998); F. Mila, Phys. Rev. Lett. **81**, 2356 (1998); M. Mambrini and F. Mila, Eur. Phys. J. B **17**, 651 (2000); K. Hida, J. Phys. Soc. Jpn. **70**, 3673 (2001); D. C. Cabra, M. D. Grynberg, P. C. W. Holdsworth, and P. Pujol, Phys.

Rev. B **65**, 094418 (2002); J. Schulenburg, A. Honecker, J. Schnack, J. Richter, and H. J. Schmidt, Phys. Rev. Lett. **88**, 167207 (2002); D. C. Cabra, M. D. Grynberg, P. C. W. Holdsworth, A. Honecker, P. Pujol, J. Richter, D. Schmalfuss, and J. Schulenburg, Phys. Rev. B **71**, 144420 (2005).

[7] L. B. Marston and C. Zeng, J. Appl. Phys. **69**, 5962 (1991); A. V. Syromyatnikov and S. V. Maleyev, Phys. Rev. B **66**, 132408 (2002); P. Nikolič and T. Senthil, *ibid.* **68**, 214415 (2003); R. Budnik and A. Auerbach, Phys. Rev. Lett. **93**, 187205 (2004); R. R. P. Singh and D. A. Huse, Phys. Rev. B **76**, 180407(R) (2007).

[8] B. Sriram Shastry and B. Sutherland, Physica B & C **108**, 1069 (1981); Zheng Weihong, C. J. Hamer, and J. Oitmaa, Phys. Rev. B **60**, 6608 (1999); S. Miyahara and K. Ueda, Phys. Rev. Lett. **82**, 3701 (1999); E. Müller-Hartmann, R. R. P. Singh, C. Knetter, and G. S. Uhrig, *ibid.* **84**, 1808 (2000); A. Koga and N. Kawakami, *ibid.* **84**, 4461 (2000); C. H. Chung, J. B. Marston, and S. Sachdev, Phys. Rev. B **64**, 134407 (2001); Y. Takushima, A. Koga, and N. Kawakami, J. Phys. Soc. Jpn. **70**, 1369 (2001); A. Läuchli, S. Wessel, and M. Sigrist, Phys. Rev. B **66**, 014401 (2002); S. Miyahara and K. Ueda, J. Phys.: Condens. Matter **15**, R327 (2003).

[9] J. Richter, J. Schulenburg, A. Honecker, and D. Schmalfusz, Phys. Rev. B **70**, 174454 (2004); G. Misguich and P. Sindzingre, J. Phys.: Condens. Matter **19**, 145202 (2007).

[10] S. E. Palmer and J. T. Chalker, Phys. Rev. B **64**, 094412 (2001); W. Brenig and A. Honecker, *ibid.* **65**, 140407 (2002); B. Canals, *ibid.* **65**, 184408 (2002); J. B. Fouet, M. Mambrini, P. Sindzingre, and C. Lhuillier, *ibid.* **67**, 054411 (2003); J. Richter, J. Schulenburg, A. Honecker, J. Schnack, and H.-J. Schmidt, J. Phys.: Condens. Matter **16**, S779 (2004).

[11] R. Siddharthan and A. Georges, Phys. Rev. B **65**, 014417 (2001); P. Tomczak and J. Richter, J. Phys. A **36**, 5399 (2003); J. Richter, O. Derzhko, and J. Schulenburg, Phys. Rev. Lett. **93**, 107206 (2004); P. Tomczak, A. Molinska, J. Richter, and J. Schulenburg, Acta Phys. Pol. A **109**, 781 (2006); J. Richter, J. Schulenburg, P. Tomczak, and D. Schmalfuss, arXiv:cond-mat/0411673 (unpublished).

[12] M. Troyer, H. Kontani, and K. Ueda, Phys. Rev. Lett. **76**, 3822 (1996); M. Troyer, M. Imada, and K. Ueda, J. Phys. Soc. Jpn. **66**, 2957 (1997); P. Tomczak, J. Schulenburg, J. Richter, and A. R. Ferchmin, J. Phys.: Condens. Matter **13**, 3851 (2001); A. Collins, J. McEvoy, D. Robinson, C. J. Hamer, and Z. Weihong, Phys. Rev. B **73**, 024407 (2006); W. Zheng, J. Oitmaa, and C. J. Hamer, *ibid.* **75**, 184418 (2007).

[13] T. Inami, Y. Ajiro, and T. Goto, J. Phys. Soc. Jpn. **65**, 2374 (1996).

[14] H. Tanaka, T. Ono, H. Aruga Katori, H. Mitamura, F. Ishikawa, and T. Goto, Prog. Theor. Phys. Suppl. **145**, 101 (2002); T. Ono, H. Tanaka, H. Aruga Katori, F. Ishikawa, H. Mitamura, and T. Goto, Phys. Rev. B **67**, 104431 (2003); T. Ono, H. Tanaka, O. Kolomiyets, H. Mitamura, T. Goto, K. Nakajima, A. Oosawa, Y. Koike, K. Kakurai, J. Klenke, P. Smeibidle, and M. Meissner, J. Phys.: Condens. Matter **16**, S773 (2004); T. Ono, H. Tanaka, T. Nakagomi, O. Kolomiyets, H. Mitamura, F. Ishikawa, T. Goto, K. Nakajima, A. Oosawa, Y. Koike, K. Kakurai, J. Klenke, P. Smeibidle, M. Meissner, and H. Aruga Katori, J. Phys. Soc. Jpn. **74**, 135 (2005); T. Ono, H. Tanaka, O. Kolomiyets, H. Mitamura, F. Ishikawa, T. Goto, K. Nakajima, A. Oosawa, Y. Koike, K. Kakurai, J. Klenke, P. Smeibidle, M. Meissner, R. Coldea, A.

D. Tennant, and J. Ollivier, Prog. Theor. Phys. Suppl. **159**, 217 (2005).

[15] L. E. Svistov, A. I. Smirnov, L. A. Prozorova, O. A. Petrenko, L. N. Demianets, and A. Ya. Shapiro, Phys. Rev. B **67**, 094434 (2003); L. A. Prozorova, L. E. Svistov, A. I. Smirnov, O. A. Petrenko, L. N. Demianets, and A. Ya. Shapiro, J. Magn. Magn. Mater. **258-259**, 394 (2003); L. E. Svistov, A. I. Smirnov, L. A. Prozorova, O. A. Petrenko, A. Micheler, N. Büttgen, A. Ya. Shapiro, and L. N. Demianets, Phys. Rev. B **74**, 024412 (2006); A. I. Smirnov, H. Yashiro, S. Kimura, M. Hagiwara, Y. Narumi, K. Kindo, A. Kikkawa, K. Katsumata, A. Ya. Shapiro, and L. N. Demianets, *ibid.* **75**, 134412 (2007).

[16] Y. Narumi, K. Katsumata, Z. Honda, J.-C. Domenge, P. Sindzingre, C. Lhuillier, Y. Shimaoka, T. C. Kobayashi, and K. Kindo, Europhys. Lett. **65**, 705 (2004); Y. Narumi, Z. Honda, K. Katsumata, J.-C. Domenge, P. Sindzingre, C. Lhuillier, A. Matsuo, K. Suga, and K. Kindo, J. Magn. Magn. Mater. **272-276**, 878 (2004).

[17] H. Kageyama, K. Yoshimura, R. Stern, N. V. Mushnikov, K. Onizuka, M. Kato, K. Kosuge, C. P. Slichter, T. Goto, and Y. Ueda, Phys. Rev. Lett. **82**, 3168 (1999); K. Onizuka, H. Kageyama, Y. Narumi, K. Kindo, Y. Ueda, and T. Goto, J. Phys. Soc. Jpn. **69**, 1016 (2000); H. Kageyama, Y. Narumi, K. Kindo, K. Onizuka, Y. Ueda, and T. Goto, J. Alloys Compd. **317-318**, 177 (2001); H. Kageyama, Y. Ueda, Y. Narumi, K. Kindo, M. Kosaka, and Y. Uwatoko, Prog. Theor. Phys. Suppl. **145**, 17 (2002).

[18] S. Michimura, A. Shigekawa, F. Iga, M. Sera, T. Takabatake, K. Ohoyama, and Y. Okabe, Physica B (Amsterdam) **378-380**, 596 (2006); S. Yoshii, T. Yamamoto, M. Hagiwara, A. Shigekawa, S. Michimura, F. Iga, T. Takabatake, and K. Kindo, J. Phys.: Conf. Ser. **51**, 59 (2006); F. Iga, A. Shigekawa, Y. Hasegawa, S. Michimura, T. Takabatake, S. Yoshii, T. Yamamoto, M. Hagiwara, and K. Kindo, J. Magn. Magn. Mater. **310**, e443 (2007).

[19] M. E. Zhitomirsky, Phys. Rev. B **67**, 104421 (2003); A. Honecker and J. Richter, Condens. Matter Phys. **8**, 813 (2005); O. Derzhko and J. Richter, Eur. Phys. J. B **52**, 23 (2006); A. Honecker and S. Wessel, Physica B (Amsterdam) **378-380**, 1098 (2006).

[20] J. E. Greedan, J. Mater. Chem. **11**, 37 (2001); A. Harrison, J. Phys.: Condens. Matter **16**, S553 (2004).

[21] R. E. Norman, N. J. Rose, and R. E. Stenkamp, J. Chem. Soc. Dalton Trans. **1987**, 2905; R. E. Norman and R. E. Stenkamp, Acta Crystallogr., Sect. C: Cryst. Struct. Commun. **46**, 6 (1990); M. Gonzalez, F. Cervantes-Lee, and L. W. ter Haar, Mol. Cryst. Liq. Cryst. Sci. Technol., Sect. A **233**, 317 (1993).

[22] S. Maruti and L. W. ter Haar, J. Appl. Phys. **75**, 5949 (1994); S. Ateca, S. Maruti, and L. W. ter Haar, J. Magn. Magn. Mater. **147**, 398 (1995).

[23] M. Mekata, M. Abdulla, T. Asano, H. Kikuchi, T. Goto, T. Morishita, and H. Hori, J. Magn. Magn. Mater. **177-181**, 731 (1998); M. Mekata, M. Abdulla, M. Kubota, and Y. Oohara, Can. J. Phys. **79**, 1409 (2001).

[24] A. P. Ramirez, Annu. Rev. Mater. Sci. **24**, 453 (1994); *Handbook on Magnetic Materials*, edited by K. H. J. Buschow (Elsevier, Amsterdam, 2001), Vol. 13, p. 423.

[25] J. Zheng and G. Sun, Phys. Rev. B **71**, 052408 (2005).

[26] Y. L. Loh, D. X. Yao, and E. W. Carlson, Phys. Rev. B **77**, 134402 (2008).

[27] L. J. de Jongh and A. R. Miedema, *Experiments on Simple Mag-*

netic Model Systems (Taylor & Francis, London, 1974); J. de Jongh and A. R. Miedema, Adv. Phys. **50**, 947 (2001); J. Yoon and E. I. Solomon, Coord. Chem. Rev. **251**, 379 (2007).

[28] S. Okubo, M. Hayashi, S. Kimura, H. Ohta, M. Motokawa, H. Kikuchi, and H. Nagasawa, Physica B (Amsterdam) **246-247**, 553 (1998).

[29] R. Natori, Y. Watabe, and Y. Natsume, J. Phys. Soc. Jpn. **66**, 3687 (1997).

[30] J. Strečka, J. Magn. Magn. Mater. **316**, e346 (2007).

[31] To simplify further description, we will further refer to Cu^{2+} ions at the trimeric and monomeric sites as to the Heisenberg and Ising spins, respectively.

[32] M. E. Fisher, Phys. Rev. **113**, 969 (1959).

[33] I. Syozi, in *Phase Transitions and Critical Phenomena*, edited by C. Domb and M. S. Green (Academic, New York, 1972), Vol. 1.

[34] I. Syozi, Prog. Theor. Phys. **6**, 306 (1951).

[35] K. Kano and S. Naya, Prog. Theor. Phys. **10**, 158 (1953).

[36] C. Domb, Adv. Phys. **9**, 149 (1960).

[37] J. Villain, R. Bidaux, J.-P. Carton, and R. Conte, J. Phys. (Paris) **41**, 1263 (1980); E. F. Shender, Sov. Phys. JETP **56**, 178 (1982); J. N. Reimers and A. J. Berlinsky, Phys. Rev. B **48**, 9539 (1993); R. Moessner, S. L. Sondhi, and P. Chandra, Phys. Rev. Lett. **84**, 4457 (2000); R. Moessner and S. L. Sondhi, Phys. Rev. B **63**, 224401 (2001).

[38] D.-X. Yao, Y. L. Loh, E. W. Carlson, and M. Ma, following paper, Phys. Rev. B **78**, 024428 (2008).